Measuring storage and loss moduli using optical tweezers: Broadband microrheology

Manlio Tassieri,[1,*] Graham M. Gibson,[2] R. M. L. Evans,[3] Alison M. Yao,[2] Rebecca Warren,[1] Miles J. Padgett,[2] and Jonathan M. Cooper[1]

[1]*Department of Electronics and Electrical Engineering, University of Glasgow, Glasgow G12 8LT, United Kingdom*
[2]*Department of Physics and Astronomy, SUPA, University of Glasgow, Glasgow G12 8QQ, United Kingdom*
[3]*School of Physics and Astronomy, University of Leeds, Leeds LS2 9JT, United Kingdom*

We present an experimental procedure to perform broadband microrheological measurements with optical tweezers. A generalized Langevin equation is adopted to relate the time-dependent trajectory of a particle in an imposed flow to the frequency-dependent moduli of the complex fluid. This procedure allows us to measure the material linear viscoelastic properties across the *widest* frequency range achievable with optical tweezers.

I. INTRODUCTION

In 1986 Ashkin and colleagues reported the first observation of what is now commonly referred to as optical tweezers: a tightly focused beam of light capable of holding microscopic particles stable in three dimensions [1]. Since then, several studies have adopted this technique as a tool for purposes as varied as trapping solid aerosols [2], measuring the viscosity of biomaterials [3,4], the forces exerted by single motor proteins [5] and the compliance of bacterial tails [6], or stretching single DNA molecules [7]. However, there remain a number of issues when optical tweezers are used for microrheological measurements.

Microrheology is a branch of rheology having the same principles as conventional bulk rheology (i.e., to study the linear viscoelastic behavior of materials), but working on micron length scales. The linear viscoelastic properties of a material can be represented by the frequency-dependent dynamic complex modulus $G^*(\omega)$, which provides information on both the viscous and the elastic nature of the material. The conventional method of measuring $G^*(\omega)$ is based on the imposition of an oscillatory stress $\sigma(\omega,t)$ and the measurement of the resulting oscillatory strain $\gamma(\omega,t)$, or vice versa. The amplitudes of its in-phase and out-of-phase components are both proportional to the stress amplitude, with constants of proportionality defining, respectively, the storage (elastic) $G'(\omega)$ and the loss (viscous) $G''(\omega)$ moduli [8].

Optical tweezers have been successfully used with Newtonian fluids for rheological purposes such as determining the fluid viscosity with a high accuracy, measuring the hydrodynamic interactions between particles, or estimating the wall effect on the Stokes drag coefficient (i.e., Faxén's correction), as reviewed in Ref. [9]. Conversely, when optical tweezers are adopted for measuring the viscoelastic properties of complex fluids the results are either limited to the material high-frequency response [10–12], discarding the essential information related to long time scale (i.e., low-frequency) material behavior, or supported by low-frequency measurements performed by different techniques (e.g., rotational rheometry [13] or passive video particle tracking

(PVPT) microrheology [14]), but either without showing a clear overlapping region between the results [13] or even leaving a macroscopic gap of information in the range of frequencies explored [14].

The aim of this work is to present a self-consistent procedure for measuring the linear viscoelastic properties of materials, from nonoscillatory measurements, across the widest frequency range achievable with optical tweezers. In particular, the procedure consists of two steps: (I) measuring the thermal fluctuations of a trapped bead for a sufficiently long time and (II) measuring the transient bead displacement, from the optical trap center, in response to a uniform fluid flow field entraining the bead. The flow is instantaneously switched on at time zero by translating the whole fluid sample while the trap is held fixed. The imposed constant-velocity motion continues until a steady displacement of the bead is reached. The analysis of step (I) provides (a) the trap stiffness (κ)—note that this has the added advantage of making the present method self-calibrated—and (b) the high-frequency viscoelastic properties of the material to a high accuracy. Step (II) has the potential to provide information about the viscoelastic properties of the material down to very low frequencies, limited only by the duration of the experiment. However, because of the harmonic nature of the optical trap, which tends not to transmit high-frequency applied forces to the bead, the material's high-frequency response cannot be determined by this step. The full material viscoelastic spectrum is thus resolved by combining the results obtained from steps (I) and (II).

II. ANALYTICAL MODEL

The experimental procedure is analytically described through the analysis of the motion of a bead trapped in a stationary harmonic potential of force constant κ, where a uniform fluid flow field of magnitude $|\vec{V}_s|$ can be exerted at time $t=0$. The equation describing the bead position $\vec{r}(t)\,\forall\,t$ can be derived by means of the generalized Langevin equation, which in three dimensions is

$$m\vec{a}(t) = \vec{f}_R(t) - \int_0^t \zeta(t-\tau)[\vec{v}(\tau) - \vec{V}_s(\tau)]d\tau - \kappa\vec{r}(t), \quad (1)$$

where m is the mass of the particle, $\vec{a}(t)$ is its acceleration, $\vec{v}(t)$ is the bead velocity, $\vec{V}_s(t)$ is the fluid flow field velocity,

*m.tassieri@elec.gla.ac.uk

and $\vec{f}_R(t)$ is the usual Gaussian white noise term, modeling stochastic thermal forces acting on the particle. The integral term represents the viscous damping of the fluid, which incorporates a generalized time-dependent memory function $\zeta(t)$.

We now show how Eq. (1) evolves in the two cases mentioned above: when $\vec{V}_s(t)=\vec{0}$ and $\vec{V}_s(t)\neq\vec{0}$, respectively. In the first case, where $\vec{V}_s(t)=\vec{0}$, the optical tweezers can be calibrated by using the principle of equipartition of energy,

$$\tfrac{3}{2}k_B T = \tfrac{1}{2}\kappa\langle r^2\rangle, \qquad (2)$$

where k_B is the Boltzmann constant, T is the absolute temperature, and $\langle r^2\rangle$ is the time-independent variance of the particle displacement from the trap center, the origin of $\vec{r}$. Despite all the possible methods for determining the optical trap stiffness (e.g., using the power spectrum or the drag force [15–17]), the equipartition method is the only method independent of the viscoelastic properties of the material under investigation and is thus essential from a rheological point of view.

The thermal fluctuations of the trapped bead can also be investigated to determine the high-frequency viscoelastic properties of the material through the analysis of the time dependence of the mean-square displacement (MSD) $\langle\Delta r^2(\tau)\rangle$,

$$\langle\Delta r^2(\tau)\rangle \equiv \langle[\vec{r}(t+\tau)-\vec{r}(t)]^2\rangle_t, \qquad (3)$$

where t is the absolute time and τ is the lag time. The average is taken over all initial times t and the number of particles considered in the experiment, if more than 1. In particular, using the assumptions adopted by Mason and Weitz in the study of the motion of thermally excited free particles [18], at thermal equilibrium, where $\langle\vec{v}(t)\vec{f}_R(t)\rangle=0$ and $m\langle\vec{v}(t)\vec{v}(t)\rangle=6k_B T\,\forall\,t$, Eq. (1) yields, in the Laplace form, the velocity autocorrelation function

$$\langle v(0)\tilde{v}(s)\rangle = \frac{6k_B T}{ms+\tilde{\zeta}(s)+\kappa/s} \equiv s^2\langle\Delta\tilde{r}^2(s)\rangle, \qquad (4)$$

where s is the Laplace frequency. Following Mason and Weitz [18] in assuming that the bulk Laplace-frequency-dependent viscosity of the fluid $\tilde{\eta}(s)$ is proportional to the microscopic memory function $\tilde{\zeta}(s)=6\pi a\tilde{\eta}(s)$, where a is the bead radius, Eq. (4) can be written as

$$\tilde{\eta}(s) = \frac{1}{6\pi a}\left[\frac{6k_B T}{s^2\langle\Delta\tilde{r}^2(s)\rangle} - ms - \frac{\kappa}{s}\right], \qquad (5)$$

where the first term in the brackets reflects the viscoelasticity of the medium, the second term is related to the inertia of the bead, and the third term takes into account the optical trap strength. It is easy to demonstrate that, for a microbead of density on order of 1 g/cm^3 suspended in water, the product ms is negligible compared with the first term for the majority of the experimentally accessible frequencies (i.e., $s \ll 10^6$ s^{-1}). With regard to the optical trap strength, two limiting cases can be distinguished: (i) in the limit $\kappa/s\rightarrow 0$, which can be obtained either for vanishing trap strength or for measurements performed at high frequencies, but lower

than 10^6 s^{-1}, Eq. (5) recovers the generalized Stokes-Einstein relationship derived by Mason and Weitz [18]; and (ii) in the limit $\kappa/s\rightarrow\infty$, which can be obtained either for a strong optical trap or for measurements performed at very low frequencies, Eq. (5) gives the same result as if the bead were embedded in a purely elastic continuum with elastic constant of $\kappa/6\pi a$. For all intermediate cases, where $0 < \kappa/s < \infty$, it is easy to show that, by analytical continuation from Eq. (5), the complex modulus can be expressed directly in terms of the time-dependent MSD,

$$G^*(\omega) = s\,\tilde{\eta}(s)|_{s=i\omega} = \frac{\kappa}{6\pi a}\left[\frac{2\langle r^2\rangle}{i\omega\langle\widehat{\Delta r^2}(\omega)\rangle} - 1\right], \qquad (6)$$

where $\langle\widehat{\Delta r^2}(\omega)\rangle$ is the Fourier transform of $\langle\Delta r^2(\tau)\rangle$.

The second step of the procedure, which experimentally follows the first, consists of the analysis of the induced bead displacement from the trap center due to an imposed time-dependent uniform fluid flow field $\vec{V}_s(t)$ entraining the bead. In this case, Eq. (1) yields, in the Laplace form, the mean velocity of the particle,

$$\langle\tilde{v}(s)\rangle = \frac{\tilde{\zeta}(s)\tilde{V}_s(s)}{ms+\tilde{\zeta}(s)+\kappa/s} \equiv s\langle\tilde{r}(s)\rangle, \qquad (7)$$

where the brackets $\langle\cdots\rangle$ denote the average over several independent measurements (but not averaged over absolute time since time-translation invariance has been broken by the flow startup at $t=0$). It is straightforward to show that, by analytical continuation from Eq. (7), the complex modulus can be expressed directly in terms of both the imposed flow field and the induced bead displacement from the trap center,

$$G^*(\omega) = s\,\tilde{\eta}(s)|_{s=i\omega} = \frac{(\kappa-m\omega^2)i\omega\langle\hat{r}(\omega)\rangle}{6\pi a[\hat{V}_s(\omega)-i\omega\langle\hat{r}(\omega)\rangle]}, \qquad (8)$$

where $\hat{V}_s(\omega)$ and $\langle\hat{r}(\omega)\rangle$ are the Fourier transforms of $\vec{V}_s(t)$ and $\langle\vec{r}(t)\rangle$, respectively. Note that, so far, the temporal form of $\vec{V}_s(t)$ is still undefined. Thus, Eq. (8) represents the general solution for $G^*(\omega)$ independently of the temporal form of $\vec{V}_s(t)$ [e.g., sinusoidal function $\vec{V}_s\sin(\omega t)$ or, as in this work, Heaviside step function $\vec{V}_s H(t)$, where $\vec{V}_s(t)=\vec{0}\,\forall\,t<0$ and $\vec{V}_s(t)=\vec{V}_s\,\forall\,t\geq 0$].

In principle, Eqs. (6) and (8) are two simple expressions relating the material complex modulus $G^*(\omega)$ to the observed time-dependent bead trajectory $\vec{r}(t)$ via the Fourier transform of either $\vec{r}(t)$ itself [in Eq. (8)] or the related MSD [in Eq. (6)]. In practice, the evaluation of these Fourier transforms, given only a finite set of data points over a finite time domain, is nontrivial since interpolation and extrapolation from those data can yield serious artifacts if handled carelessly.

In order to express the two Fourier transforms in Eqs. (6) and (8) in terms of the N experimental data points $[t_k,\langle\Delta r^2(\tau)\rangle_k]$ and $[t_k,\langle\vec{r}(t)\rangle_k]$, respectively, where $k=1,\ldots,N$, which extend over a finite range, exist only for positive t, and *need not* to be equally spaced, we adopt the analytical method introduced in Ref. [19]. In particular, we refer to Eq. (10) of Ref. [19], which is equally applicable to find the Fourier transform $\hat{g}(\omega)$ of any time-dependent quan-

tity $g(t)$ sampled at a finite set of data points (t_k, g_k), giving

$$-\omega^2 \hat{g}(\omega) = i\omega g(0) + (1 - e^{-i\omega t_1}) \frac{[g_1 - g(0)]}{t_1} + \dot{g}_\infty e^{-i\omega t_N}$$

$$+ \sum_{k=2}^{N} \left(\frac{g_k - g_{k-1}}{t_k - t_{k-1}} \right) (e^{-i\omega t_{k-1}} - e^{-i\omega t_k}), \qquad (9)$$

where $\dot{g}_\infty$ is the gradient of $g(t)$ extrapolated to infinite time. Also $g(0)$ is the value of $g(t)$ extrapolated to $t=0^+$. Identical formulas can be written for both $\langle \widehat{\Delta r^2}(\omega) \rangle$ and $\langle \hat{r}(\omega) \rangle$, with g being replaced with $\langle \Delta r^2 \rangle$ and $\langle \vec{r} \rangle$, respectively. This analytical procedure has the advantage of removing the need for Laplace and inverse-Laplace transformations of experimental data [20].

III. EXPERIMENTAL DETAILS

We have tested Eqs. (6) and (8), via Eq. (9), by measuring both the viscosity of water and the viscoelastic properties of water-based solutions of polyacrylamide (PAM, flexible polyelectrolytes, $M_w = 5 \times 10^6$–6×10^6 g/mol, Polysciences, Inc.) using optical tweezers as described below. Trapping is achieved using a cw Ti:sapphire laser system (M Squared, SolsTiS) which provides up to 1 W at 830 nm. The tweezers are based around an inverted microscope, where the same objective lens (100×, 1.3 numerical aperture, Zeiss, Plan-Neofluor) is used both to focus the trapping beam and to image the resulting motion of the particles. Samples are mounted in a motorized microscope stage (ASI, MS-2000). Two complementary metal-oxide semiconductor cameras are used to view the sample, with bright-field illumination: one provides a wide field of view (Prosilica EC1280M), while the other takes high-speed images of a reduced field of view (Prosilica GV640M). These images are processed in real time at 2 kHz using our own LABVIEW (National Instruments) particle tracking software running on a standard desktop PC [21].

IV. RESULTS

The Brownian fluctuations of an optically trapped bead give rise to the time-dependent $\langle \Delta r^2(\tau) \rangle$ shown in Fig. 1. In the case of a bead immersed in a Newtonian fluid, it is expected that at short time intervals (thus small distances) the bead behaves as if it were free to diffuse. Indeed, the agreement between the observed $\langle \Delta r^2(\tau) \rangle$ at short times of a trapped bead in water (circles) and the Einstein prediction for a freely diffusing bead (solid line) is good. As the time intervals increase the bead becomes influenced by the optical potential. This results in a plateau at large time intervals, where $\langle \Delta r^2(\tau) \rangle$ tends to $2\langle r^2 \rangle$. It is interesting to note that the ratio of these two quantities (the MSD and twice the variance of the positional distribution) is a dimensionless parameter, independent of both the optical trap stiffness and the bead radius. It thus allows an explicit comparison between the dynamics of the fluids under investigation as shown in Fig. 2. Moreover, the onset point of the plateau region in Fig. 2 indicates the bottom limit of the frequency range within
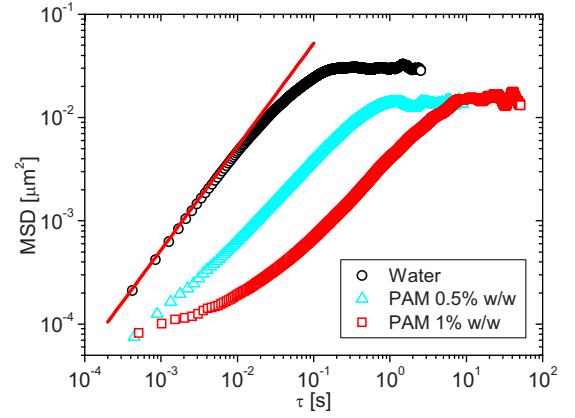

FIG. 1. (Color online) The MSD vs lag time of a 5-μm-diameter bead in water (with $\kappa = 0.8$ μN/m) and in two water-based solutions of PAM at concentrations of 0.5% and 1% w/w (both with $\kappa = 1.7$ μN/m). The line is the Einstein prediction of the MSD for a 5-μm-diameter bead in water at 25 °C.

which the moduli can be determined by Eq. (6), as for all the previous works using stationary optical tweezers.

In Fig. 3 we compare the responses of a 5-μm-diameter bead immersed in water (a Newtonian fluid) and in a water solution of PAM at 1% w/w (a non-Newtonian fluid) due to the imposition of a uniform fluid flow field having temporal behavior as a Heaviside step function $\vec{V}_s(t) = \vec{V}_s H(t)$, with different magnitudes in the two measurements. Experimentally, the execution of a Heaviside step function is achieved by suddenly moving the motorized microscope stage at a predetermined speed and direction (here, parallel to the x axis). The experiment runs until a steady displacement (Δx) of the bead from the trap center is reached (i.e., until all the material's characteristic relaxation times are exceeded). In Fig. 3 the x component of the bead displacement has been normalized by Δx for a better comparison between the viscoelastic characters of the two samples. It is clear that while the Newtonian fluid reaches a steady value of the displacement almost *instantaneously* (as expected), the non-Newtonian fluid shows complex dynamics representative of its viscoelastic
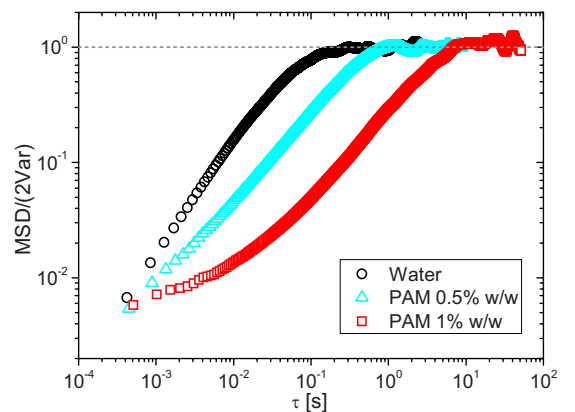

FIG. 2. (Color online) The normalized MSD vs lag time of a 5-μm-diameter bead in water (with $\kappa = 0.8$ μN/m) and in two water-based solutions of PAM at concentrations of 0.5% and 1% w/w (both with $\kappa = 1.7$ μN/m).
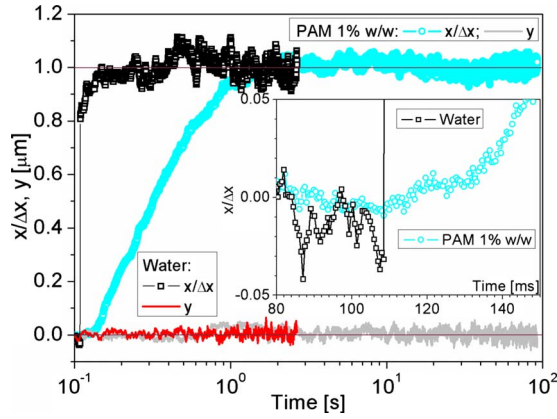
FIG. 3. (Color online) The coordinates of a 5-μm-diameter bead vs time for two different solutions and for two uniform fluid flow fields of different magnitudes $|\vec{V}_s|$ at 25 °C. In both cases the data were averaged over three measurements and the x coordinate has been normalized by the steady-state displacement Δx. In water κ =1.7 μN/m, $|\vec{V}_s|$=20 μm/s, and Δx=0.523 μm. In 1% w/w of PAM κ=8.6 μN/m, $|\vec{V}_s|$=3 μm/s, and Δx=1.155 μm. The inset highlights the startup behavior of both the above systems.

nature. It is important at this point to note that, because of the harmonic nature of the optical potential, at early times (i.e., for $t \to 0$ or equivalently for $\omega \to \infty$), the trapping force exerted on the bead is actually small [i.e., $\kappa \vec{r}(t) \to 0$] and the particle moves almost at the same speed as the imposed flow [i.e., $\vec{v}(t) \cong \vec{V}_s(t)$]; this implies that Eq. (8) becomes undefined at high frequencies.

The broadband microrheological measurement with optical tweezers is achieved by combining the frequency responses obtained from both the methods introduced above. In particular, the material's high-frequency response is determined by applying Eq. (6) [via Eq. (9) with $\langle \Delta r^2 \rangle_k$ replacing g_k] to the $\langle \Delta r^2(\tau) \rangle$ measurements, whereas the low-frequency response is resolved by applying Eq. (8) [via Eq. (9) with $\langle \vec{r} \rangle_k$ replacing g_k] to the data describing the bead's transient response to the motion of the stage.
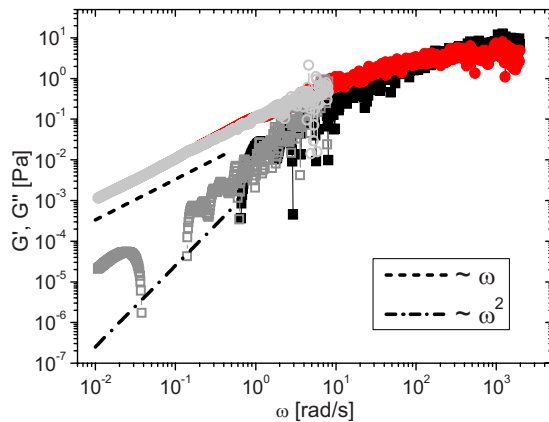

FIG. 4. (Color online) Storage (squares) and loss (circles) moduli vs frequency of a solution of 1% w/w of PAM in water measured by means of both Eq. (6) (solid symbols at high frequencies) and Eq. (8) (open symbols at low frequencies) applied directly to the experimental data presented in Figs. 2 and 3, respectively.
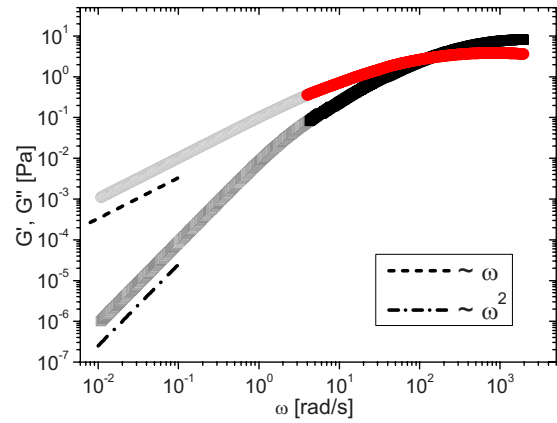

FIG. 5. (Color online) Storage (squares) and loss (circles) moduli vs frequency of a solution of 1% w/w of PAM in water measured by means of both Eq. (6) (solid symbols at high frequencies) and Eq. (8) (open symbols at low frequencies) applied directly to the experimental data presented in Figs. 2 and 3, but smoothed.

A typical result of this procedure for a non-Newtonian fluid is shown in Fig. 4 while, in the case of water, a constant viscosity of $\eta = 8.69 \times 10^{-4} \pm 6 \times 10^{-6}$ Pa s is measured over five frequency decades at 25 °C. It is evident that, although there is some noise in the frequency domain that has propagated from genuine experimental noise in the time-domain data, there is a clear overlapping region of agreement between the two methods that makes the whole procedure self-consistent. Moreover, it confirms the ease with which the low-frequency material response can be explored, right down to the terminal region (where $G' \propto \omega^2$ and $G'' \propto \omega$), which is the current limitation for microrheological measurements performed not only with stationary optical tweezers (as shown here by the high-frequency response in Fig. 4, limited to frequencies above 10^0 s^{-1}), but also with PVPT and diffusing wave spectroscopy [22]. In particular, in PVPT microrheological measurements, the lowest accessible frequency is inversely proportional to both the fluid viscosity and the bead size; it is given by the inverse of the longest time for which the probe particle stays in focus (i.e., within the objective depth of field) during the experiment. For example, in water at 25 °C a micron-sized bead, observed through a 100$\times$ objective with a depth of field of order 200 nm, would remain in focus for a time of order 0.1 s. The experimental method presented here, on the other hand, has no fundamental restriction on the lowest achievable frequency. Indeed, with a suitable choice of the velocity of the applied fluid flow field (e.g., $|\vec{V}_s|$=3 μm/s) and the sample holder geometry (e.g., a 3-cm-long microfluidic channel), an experiment could be made to run for hours, thereby probing frequencies of order 10^{-4} s^{-1} or lower, without limit. Finally, in order to remove the genuine noise, a simple smoothing operation of the original data is sufficient and the results are shown in Fig. 5.

V. CONCLUSIONS

In summary, we have presented a self-consistent and simple experimental procedure, coupled with an analytical

data analysis method, for determining the broadband viscoelastic properties of complex fluids with optical tweezers. This method extends the range of the frequency response achieved by conventional optical tweezers measurements down to the material's terminal region. In fact, the method has no lower limit on the accessible frequency, thus allowing microrheological measurements to be performed on complex fluids with very long relaxation times, such as those exhibiting soft glassy rheology [23], or composed of very high molecular weight polymers. Thus, the accessible frequency spectrum for small samples of complex fluids is now limited only by the patience of the observer.

[1] A. Ashkin, J. M. Dziedzic, J. E. Bjorkholm, and S. Chu, Opt. Lett. **11**, 288 (1986).

[2] M. D. Summers, D. R. Burnham, and D. McGloin, Opt. Express **16**, 7739 (2008).

[3] P. A. Negulescu, T. B. Krasieva, A. Khan, H. H. Kerschbaum, and M. D. Cahalan, Immunity **4**, 421 (1996).

[4] K. Svoboda, C. F. Schmidt, D. Branton, and S. M. Block, Biophys. J. **63**, 784 (1992).

[5] J. T. Finer, R. M. Simmons, and J. A. Spudich, Nature (London) **368**, 113 (1994).

[6] S. M. Block, H. C. Blair, and H. C. Berg, Nature (London) **338**, 514 (1989).

[7] W. D. Wang, H. Yin, R. Landick, J. Gelles, and S. M. Block, Biophys. J. **72**, 1335 (1997).

[8] J. D. Ferry, *Viscoelastic Properties of Polymers*, 3rd ed. (Wiley, New York, 1980).

[9] A. M. Yao, M. Tassieri, M. J. Padgett, and J. M. Cooper, Lab Chip **9**, 2568 (2009).

[10] L. Starrs and P. Bartlett, J. Phys.: Condens. Matter **15**, S251 (2003).

[11] M. Atakhorrami and C. F. Schmidt, Rheol. Acta **45**, 449 (2006).

[12] N. Nijenhuis, D. Mizuno, J. A. E. Spaan, and C. F. Schmidt, Phys. Biol. **6**, 025014 (2009).

[13] G. Pesce, A. C. De Luca, G. Rusciano, P. A. Netti, S. Fusco, and A. Sasso, J. Opt. A, Pure Appl. Opt. **11**, 034016 (2009).

[14] I. M. Tolić-Nørrelykke, E.-L. Munteanu, G. Thon, L. Oddershede, and K. Berg-Sørensen, Phys. Rev. Lett. **93**, 078102 (2004).

[15] K. Berg-Sørensen and H. Flyvbjerg, Rev. Sci. Instrum. **75**, 594 (2004).

[16] K. C. Neuman and S. M. Block, Rev. Sci. Instrum. **75**, 2787 (2004).

[17] S. F. Tolić-Nørrelykke, E. Schäffer, J. Howard, F. S. Pavone, F. Jülicher, and H. Flyvbjerg, Rev. Sci. Instrum. **77**, 103101 (2006).

[18] T. G. Mason and D. A. Weitz, Phys. Rev. Lett. **74**, 1250 (1995).

[19] R. M. L. Evans, M. Tassieri, D. Auhl, and T. A. Waigh, Phys. Rev. E **80**, 012501 (2009).

[20] T. G. Mason, K. Ganesan, J. H. van Zanten, D. Wirtz, and S. C. Kuo, Phys. Rev. Lett. **79**, 3282 (1997).

[21] G. M. Gibson, J. Leach, S. Keen, A. J. Wright, and M. J. Padgett, Opt. Express **16**, 14561 (2008).

[22] T. A. Waigh, Rep. Prog. Phys. **68**, 685 (2005).

[23] S. M. Fielding, P. Sollich, and M. E. Cates, J. Rheol. **44**, 323 (2000).